Population pulsations and nondegenerate four-wave mixing in semiconductor lasers and amplifiers

Govind P. Agrawal

AT&T Bell Laboratories, Murray Hill, New Jersey 07974

Received June 8, 1987; accepted September 14, 1987

The theory of nondegenerate four-wave mixing (NDFWM) in semiconductor lasers and amplifiers is presented with particular emphasis on the physical processes that lead to population pulsations. In the case of nearly degenerate four-wave mixing, modulation of the carrier density at the beat frequency Ω of the pump and probe waves creates a dynamic population grating whose effectiveness is governed by the spontaneous carrier lifetime τ_s. Such a grating affects both the gain and the refractive index of the probe wave. In particular, the probe gain exhibits features analogous to those observed in a detuned atomic system arising from the optical Stark effect. Both the gain grating and the index grating contribute to NDFWM, with the dominant contribution coming from the index grating. For detunings such that $\Omega\tau_s \gg 1$, population pulsations correspond to modulation of the intraband population arising from spectral hole burning. Our results show that NDFWM is then limited by the phase-mismatch effects governed by the transit time τ rather than by the intraband population-relaxation time T_1. Significant NDFWM is expected to occur for detunings up to about 300 GHz for typical transit-time values of 3 psec in semiconductor lasers.

1. INTRODUCTION

The phenomenon of four-wave mixing has been studied extensively in recent years, particularly in relation to its application to optical phase conjugation.[1–3] The previous work on degenerate four-wave mixing in atomic, molecular, and semiconductor media is reviewed in Ref. 1. In most nonlinear media, the poor efficiency of the four-wave mixing process is often the limiting factor. Two ways to enhance the efficiency are (1) the use of an intracavity geometry[4–6] and (2) the use of an amplifying nonlinear medium rather than an absorbing one.[7–9] Semiconductor lasers are attractive, since both of these features are available in a compact device. More specifically, the cleaved facets form a Fabry–Perot cavity leading to an intracavity geometry, whereas the electrical pumping provides an amplifying semiconductor medium at relatively low currents (~10 mA). Furthermore, the pump beams can be generated internally by pumping the semiconductor laser above its threshold. Indeed, recent experiments demonstrated that nondegenerate four-wave mixing (NDFWM) inside a semiconductor laser can be highly efficient at pump powers of only a few milliwatts.[10–12]

The initial attempts to understand the experimental results modeled the semiconductor-laser medium as an inverted two-level system.[13,14] Such an approach, although capable of explaining the qualitative behavior, has several limitations. To mention a few, (1) the parameters of the two-level system cannot be related directly to the known device parameters, (2) spatial effects related to the laser waveguide are not accounted for, and (3) the effects of carrier-induced index changes are not included. The last limitation is particularly important for semiconductor lasers, in which a change in the carrier population (electrons or holes) affects not only the optical gain but also the refractive index. In a recent letter[15] I outlined a theory of NDFWM in semiconductor laser media that accounts properly for these effects. The objective of this paper is to provide a comprehensive account of the theory with particular attention being paid to the phenomenon of population pulsations in semiconductor lasers and amplifiers.

Population pulsations were first studied in the context of multimode gas lasers[16,17] and have recently been used to explain the dynamic instabilities of single-mode lasers.[18] Bogatov *et al.*[19] were apparently the first authors to point out that the inclusion of population pulsations (modulation of the carrier density) leads to an asymmetric interaction between the longitudinal modes of a semiconductor laser. As we shall see, the same effect is at the origin of NDFWM in semiconductor lasers. More specifically, modulation of the carrier density at the beat frequency $\Omega = \omega_1 - \omega_0$ of the pump and probe waves creates gain and index gratings. Diffraction of the counterpropagating pump wave from these dynamic gratings generates a conjugate wave at $\omega_2 = 2\omega_0 - \omega_1$. The effectiveness of the gratings is governed by the spontaneous carrier lifetime ($\tau_s \simeq$2–3 nsec). Since the carrier density cannot be modulated at frequencies much higher than τ_s^{-1}, NDFWM ceases to occur when the pump–probe detuning exceeds a few gigahertz ($|\Omega|\tau_s \gg 1$).

For semiconductor lasers, however, an additional mechanism of population pulsations should be considered; it can lead to significant NDFWM even when the pump–probe detuning exceeds 100 GHz.[20] The physical phenomenon behind highly NDFWM is spectral hole burning,[21,22] manifested as a nonlinear reduction of the optical gain by a few percent at operating powers of a few milliwatts.[23–26] Spectral hole burning is governed by the intraband relaxation processes occurring at a fast time scale (typically <1 psec). As a result, the dynamic gain and index gratings remain an effective source of NDFWM for beat frequencies of $\Omega \sim 1$ THz. The important point to note is that population pulsations in this context do not refer to actual modulation of the carrier density but rather to modulation of the occupation probability of carriers within a band. In other words, even though the intraband population pulsates, the carrier density is unable to respond to such pulsations because of the relatively slow interband recombination processes governed

0740-3224/88/010147-13$02.00

by the spontaneous carrier lifetime τ_s. Nonetheless, the resulting gain and index gratings can lead to efficient NDFWM.

The theory of NDFWM is developed by using the density-matrix approach, in which the semiconductor medium is modeled as an ensemble of collision-broadened two-level systems.[23-26] Even though there is some concern about the validity of the Bloch equations in solids, we assume that the dynamics of each two-level system is described well by them. In general, modulation of both the interband and the intraband populations should be considered for an accurate description of NDFWM. However, depending on the amount of pump–probe detuning, the analysis can be simplified in the two limiting cases. For $|\Omega|\tau_s \gg 1$, the interband modulation can be ignored, as the carrier density cannot respond at such fast time scales. For $|\Omega|\tau_s \lesssim 1$, the interband effects dominate over the intraband modulation, and the latter can be neglected.

This paper is organized as follows. In Section 2 we consider the case of nearly degenerate four-wave mixing in which the pump–probe detuning is relatively small ($|\Omega|\tau_s < 1$). It is then possible to employ the rate-equation approximation. Population pulsations are taken into account by solving the carrier-density rate equation with a time-dependent term oscillating at the beat frequency Ω. The general formalism presented in Section 2 permits us to consider the nonlinear interaction among pump, probe, and conjugate waves inside the active region of a semiconductor laser and to obtain the induced polarization at their respective frequencies. In Section 3 we consider the optical Stark effect, and we obtain the probe susceptibility and study how it is affected by the intense pump wave. Both the probe gain and the probe index are affected by the pump wave. In particular, the probe gain is considerably enhanced for specific values of pump–probe detunings.

In Section 4 we give the theory of nearly degenerate four-wave mixing, and we obtain the coupled-wave equations for the probe and conjugate waves. These equations are solved for the specific case of a semiconductor laser operating below threshold as a traveling-wave amplifier. Because of the amplifying nature of the nonliner medium, a conjugate reflectivity in the range of 100–1000 can easily be obtained at incident pump powers of about 1 mW. Population pulsations lead to considerable enhancement of the probe transmittance for detunings such that $|\Omega|\tau_s \lesssim 1$. We discuss in detail the spectral features arising from population pulsations both for the conjugate reflectivity and for the probe transmittivity. In Section 5 we consider highly NDFWM and show that the modulation of intraband modulation in semiconductor lasers can generate conjugate waves even for pump–probe detunings exceeding 100 GHz. The range of detunings in this case is limited by the phase mismatch rather than by the medium response time. Finally, the results are summarized in Section 6.

2. GENERAL FORMALISM

In this section we present the theory behind the nearly degenerate four-wave mixing in semiconductor lasers. Only collinear geometry is considered, since the thin active region (~0.1–0.2 μm) of semiconductor lasers requires that the pump, probe, and conjugate waves propagate parallel to one another in order to maximize the interaction length. We assume that the laser structure supports only the fundamental waveguide TE mode with the transverse distribution $U(x, y)$. This is generally the case for strongly index-guided lasers employing a buried-heterostructure design.[27] If all fields remain linearly polarized during their interaction, the propagation characteristics can be obtained by solving the scalar wave equation

$$\nabla^2 E - \frac{n^2}{c^2}\frac{\partial^2 E}{\partial t^2} = \frac{1}{\epsilon_0 c^2}\frac{\partial^2 P}{\partial t^2}, \tag{2.1}$$

where n is the refractive index, ϵ_0 is the vacuum permittivity, and c is the velocity of light in vacuum. The total intracavity field E is given by

$$E(x, y, z, t) = U(x, y)\sum_j E_j(z)\exp(-i\omega_j t), \tag{2.2}$$

where $j = 0, 1, 2$ for pump, probe, and conjugate waves, respectively.

The evaluation of the induced polarization P is in general fairly involved and requires knowledge of the band-structure details. In the density-matrix approach,[23-26] each pair of the conduction-band and valence-band states participating in band-to-band transitions is modeled as a two-level system, and P is calculated by summing over all possible pairs with an appropriate density of states. Although such a detailed description is necessary for the discussion of NDFWM resulting from spectral hole burning (see Section 5), a simple model can be used when the pump–probe detuning

$$\Omega = \omega_1 - \omega_0 = \omega_0 - \omega_2 \tag{2.3}$$

is relatively small, so that $|\Omega|\tau_s \lesssim 1$, where τ_s is the spontaneous carrier lifetime. In this model, the induced polarization is calculated by using

$$P = \epsilon_0 \chi(N) E, \tag{2.4}$$

where the susceptibility[27]

$$\chi(N) = -\frac{nc}{\omega_0}(\beta + i)g(N) \tag{2.5}$$

and the gain is assumed to vary linearly with the carrier density N, i.e.,

$$g(N) = a(N - N_0). \tag{2.6}$$

Here a is the gain coefficient ($a \simeq 2\times10^{-16}$ to 3×10^{-16} cm^2), and N_0 is the carrier density at which the active region becomes transparent ($N_0 \simeq 1\times10^{18}$ to 2×10^{18} cm^{-3}). The parameter β in Eq. (2.5) accounts for the carrier-induced index change that occurs invariably whenever the gain changes. It is often referred to as the linewidth enhancement factor and has typical values in the range 3–6 depending on the operating wavelength of the semiconductor lasers.[27-29]

The physical origin of the carrier-index change is related to the asymmetric nature of the gain spectrum in the semiconductor laser. For other laser systems that have a symmetric gain profile, $\beta = 0$. This feature distinguishes semiconductor lasers from gas and solid-state lasers.

The carrier density N at an injected current I is obtained by solving the rate equation

$$\frac{dN}{dt} = \frac{I}{qV} - \frac{N}{\tau_s} - \frac{g(N)}{\hbar\omega_0}|E|^2 + D\nabla^2 N, \tag{2.7}$$

where q is the electron change, V is the active volume, and D is the diffusion coefficient. Equation (2.7) can be derived from the density-matrix equations (see Section 5) in the rate-equation approximation.[23] We have assumed for simplicity that the gain $g(N)$ is the same for all waves, an assumption justified since the pump–probe detuning is much smaller compared with the gain-spectrum bandwidth ($|\Omega|T_2 \ll 1$). The solution of Eq. (2.7) is complicated because of the diffusion term. The main effect of carrier diffusion is to wash out spatial holes burned by the counterpropagating waves, as the diffusion length ($\sqrt{D\tau_s} \sim 2$–$3\ \mu$m) is much larger than the half-wavelength λ/n. Carrier diffusion in the transverse dimensions is restricted, since the transverse waveguide dimensions are generally smaller than the diffusion length. Thus, to a good degree of approximation, N can be assumed to be spatially homogeneous, satisfying the simpler rate equation

$$\frac{dN}{dt} = \frac{I}{qV} - \frac{N}{\tau_s} - \frac{g(N)}{\hbar\omega_0}\langle|E|\rangle^2, \tag{2.8}$$

where angle brackets denote the averaging operation over the active volume.

To solve Eq. (2.8), we substitute E and $g(N)$ from Eqs. (2.2) and (2.6) and assume an approximate solution of the form

$$N(t) = \overline{N} + [\Delta N \exp(-i\Omega t) + \text{c.c.}], \tag{2.9}$$

where $\overline{N}$ is the static carrier density and ΔN accounts for population pulsations. The solution of Eq. (2.8) yields the following expressions[30] for $\overline{N}$ and ΔN:

$$\overline{N} = \frac{I(\tau_s/qV) + N_0|\overline{E}_0|^2/P_s}{1 + |\overline{E}_0|^2/P_s}, \tag{2.10}$$

$$\Delta N = -\frac{C(\overline{N} - N_0)(E_0{}^*E_1 + E_0E_2{}^*)/P_s}{(1 + |\overline{E}_0|^2/P_s - i\Omega\tau_s)}, \tag{2.11}$$

where the overbar denotes averaging in the z direction,

$$P_s = \hbar\omega_0/(\Gamma a\tau_s) \tag{2.12}$$

is the saturation intensity (~1 MW/cm^2), and

$$\Gamma = \frac{\int_0^w\int_0^d |U(x, y)|^2 dx\, dy}{\int\int_{-\infty}^{\infty} |U(x, y)|^2 dx\, dy}. \tag{2.13}$$

Γ represents the fraction of mode energy confined within the active region of width w and thickness d and is often referred to as the confinement factor.[27] The overlap factor C is introduced phenomenologically and results from the non-plane-wave nature of the waveguide mode in semiconductor lasers.[19] Typically, $\Gamma = 0.3$–0.5 and $C = 0.5$–1.

The induced polarization P is calculated by using Eqs. (2.4)–(2.6) with E and N given by Eqs. (2.2) and (2.9). It is convenient to expand P into its frequency components in a manner similar to that of Eq. (2.2), i.e.,

$$P(x, y, z, t) = U(x, y) \sum_j P_j(z) \exp(-i\omega_j t). \tag{2.14}$$

We then obtain

$$P_0(z) = \epsilon_0 A g(\overline{N}) E_0(z), \tag{2.15}$$

$$P_1(z) = \epsilon_0 A [g(\overline{N}) E_1(z) + a\Delta N E_0(z)], \tag{2.16}$$

$$P_2(z) = \epsilon_0 A [g(\overline{N}) E_2(z) + a\Delta N E_0{}^*(z)], \tag{2.17}$$

where

$$A = -(nc/\omega_0)(\beta + i) \tag{2.18}$$

and

$$g(\overline{N}) = a(\overline{N} - N_0) = \frac{(a\tau_s/qV)I - aN_0}{1 + |\overline{E}_0|^2/P_s} \tag{2.19}$$

is the gain experienced by the optical fields when the current I is injected into the active region of the semiconductor laser.

This completes the general formalism. For its application we should determine whether the laser is operating below or above threshold. The threshold condition of a semiconductor laser is given by[27]

$$\Gamma g(\overline{N}) = g_{\text{th}} = \alpha_{\text{m}} + \alpha_{\text{int}}, \tag{2.20}$$

where g_{th} is the threshold gain of the lasing mode, α_{int} is the internal loss, and

$$\alpha_m = \frac{1}{2L}\ln\left(\frac{1}{R_1R_2}\right) \tag{2.21}$$

is the mirror loss for a cavity of length L and facet reflectivities R_1 and R_2. Using Eqs (2.19) and (2.20), the average intracavity pump intensity in the above-threshold regime is given by

$$\frac{|\overline{E}_0|^2}{P_s} = \frac{g_0}{g_{\text{th}}} - 1 = \frac{I - I_{\text{th}}}{I_{\text{th}} - I_0}, \tag{2.22}$$

where the small-signal gain is

$$g_0 = \Gamma a\overline{N}_0(I/I_0 - 1), \tag{2.23}$$

the threshold current is

$$I_{\text{th}} = I_0 + qVg_{\text{th}}/(a\Gamma\tau_s), \tag{2.24}$$

and

$$I_0 = qVN_0/\tau_s \tag{2.25}$$

is the current needed to achieve transparency. At $I = I_0$ the carrier density $\overline{N}_0$ just overcomes the material loss; population inversion occurs for $I > I_0$. At $I = I_{\text{th}}$ the small-signal gain is large enough to balance the cavity losses, and the laser starts to oscillate.

Equations (2.16) and (2.17) show that the induced polarization for the probe and conjugate waves has an additional contribution resulting from population pulsations (the term proportional to ΔN). This term is responsible for the enhanced probe gain as well as for four-wave mixing. We consider the two phenomena separately in Sections 3 and 4.

3. EFFECT OF POPULATION PULSATIONS ON THE PROBE GAIN

When an intense pump wave propagates in a nonlinear medium, it can modify the medium's response to the extent that the propagation characteristics of a weak probe become dependent on the pump intensity. In particular, the probe may experience gain even in an absorbing medium for specific pump–probe detunings whose values depend on the pump intensity. This effect is related to the optical Stark effect and has been well studied in the context of atomic systems.[30–33] In this section we study how the refractive index and the gain coefficient of a probe wave are affected by the intense pump propagating inside the semiconductor laser. If the laser is operating above threshold, the lasing mode plays the role of the pump, and only the probe needs to be injected from outside.

To obtain the induced polarization at the probe frequency, we substitute ΔN from Eq. (2.11) into Eq. (2.16) and obtain

$$P_1 = \epsilon_0(\chi_p E_1 + \chi_{\rm FWM} E_2^*), \tag{3.1}$$

where

$$\chi_p = Ag(\overline{N})\left(1 - \frac{CP_0}{1 + P_0 - i\Omega\tau_s}\right), \tag{3.2}$$

$$\chi_{\rm FWM} = -Ag(\overline{N})\frac{C(E_0^2/P_s)}{1 + P_0 - i\Omega\tau_s}. \tag{3.3}$$

$\chi_{\rm FWM}$ is responsible for NDFWM as discussed in Section 4. Here we discuss the qualitative and quantitative features of χ_p. In Eq. (3.2) the pump intensity

$$P_0 = |E_0|^2/P_s \tag{3.4}$$

is normalized to the saturation intensity P_s for simplicity of discussion. The probe susceptibility χ_p changes the dielectric constant at the probe frequency by $\Delta\epsilon$, which can be used to calculate the index change Δn and the probe gain g_p by using the relation

$$\chi_p = \Delta\varepsilon = 2n[\Delta n - ig_p(c/2\omega_0)]. \tag{3.5}$$

Note that g_p is the small-signal gain of the probe wave in the presence of the pump. Using Eqs. (2.18), (3.2), and (3.5), we obtain

$$\Delta n = \Delta n_0\left[1 - \frac{CP_0(1 + P_0 - \Omega\tau_s/\beta)}{(1 + P_0)^2 + (\Omega\tau_s)^2}\right], \tag{3.6}$$

$$g_p = g(\overline{N})\left[1 - \frac{CP_0(1 + P_0 + \beta\Omega\tau_s)}{(1 + P_0)^2 + (\Omega\tau_s)^2}\right], \tag{3.7}$$

where $\Delta n_0 = -\beta g(\overline{N})(c/2\omega_0)$ is the carrier-induced index change associated with the gain $g(\overline{N})$. The second term inside the square brackets in Eqs. (3.6) and (3.7) has its origin in population pulsations. To illustrate how the pump wave modifies the index change Δn and the probe gain g_p, Figs. 1 and 2 show their variation with the pump–probe detuning $\Omega\tau_s$ for several pump intensities P_0 with $\beta = 5$ and $C = 0.5$.

As Fig. 1 clearly shows, the probe gain g_p has an asymmetric line shape. More specifically, g_p is enhanced compared with its value $g(\overline{N})$ for $\Omega < 0$ and is reduced for $\Omega > 0$. An enhancement of 50% is predicted when the pump intensity equals the saturation intensity ($P_0 = 1$). Both the location and the amplitude of the gain maximum change with the pump intensity P_0. The detuning Ω_p corresponding to the maximum gain can be found by setting $dg_p/d\Omega = 0$. Using Eq. (3.7), we obtain

$$\Omega_p = -\frac{1 + P_0}{\beta\tau_s}[(1 + \beta^2)^{1/2} + 1]. \tag{3.8}$$

The index change Δn is, by contrast, reduced, with the maximum reduction occurring near $\Omega = 0$ (see Fig. 2).

The physical origin of the asymmetric line shape of the probe gain is related to the fact that a change in carrier density affects both the gain and the index of the active region in semiconductor lasers. Thus population pulsations create the gain and index gratings simultaneously; the rela-

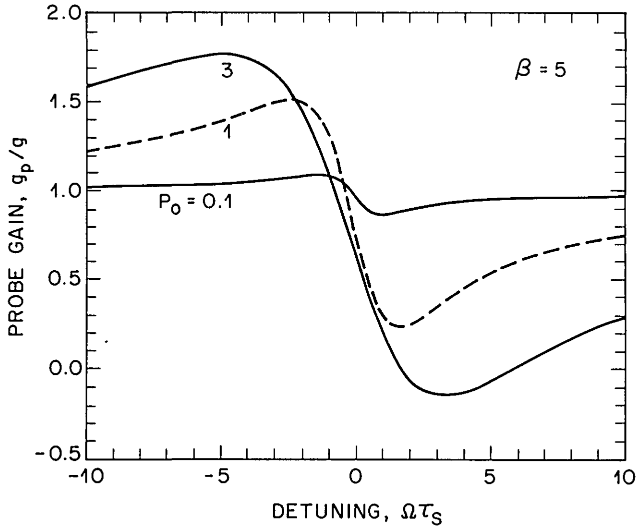

Fig. 1. Variation of the probe gain (normalized to its value expected in the absence of the pump wave) with the normalized pump–probe detuning $\Omega\tau_s$ for several pump intensities P_0 (normalized to the saturation intensity). For $\tau_s = 2$ nsec, $\Omega\tau_s = 1$ corresponds to a detuning of about 80 MHz.

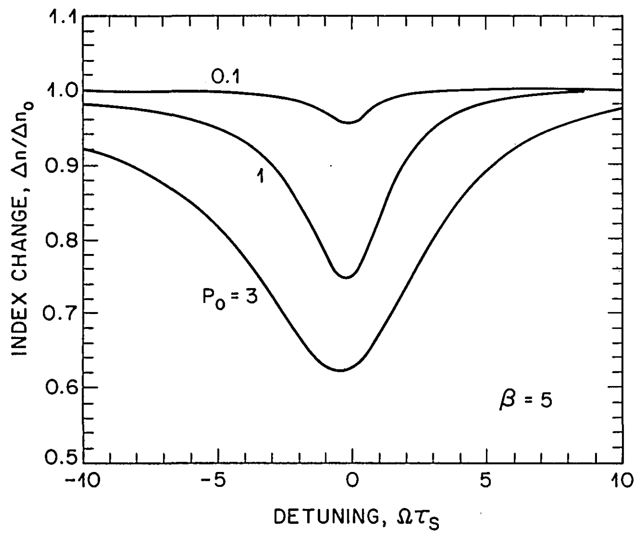

Fig. 2. Variation of the index change (normalized to its value expected in the absence of the pump wave) with the normalized pump–probe detuning $\Omega\tau_s$ for several pump intensities.

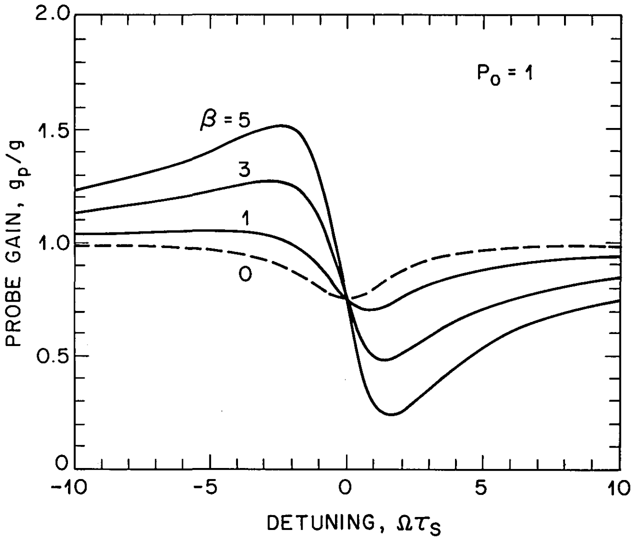

Fig. 3. Effect of the linewidth enhancement factor β on the probe-gain spectrum at a fixed pump intensity equal to the saturation intensity ($P_0 = 1$).

tive contributions of the two gratings are governed by the linewidth enhancement factor β. To see how this parameter affects the probe gain, in Fig. 3 we have shown the probe-gain spectra for several values of β at a fixed pump intensity ($P_0 = 1$). For $\beta = 0$, the index-grating contribution vanishes; the resulting line shape is symmetric, with a dip at $\Omega = 0$. For nonzero values of β, the line shape becomes asymmetric, with the maximum gain occurring at Ω_p given by Eq. (3.8). The increase in the peak height is due to an increasingly large contribution of the index grating. The relative contribution of the index grating varies as $\beta\Omega\tau_s/(1 + P_0)$, as shown by Eq. (3.7), and can significantly exceed that of the gain grating for certain values of the detunings Ω.

It is interesting to compare the probe-gain characteristics in semiconductor lasers with those expected for two-level systems.[31–34] Of particular interest is the case of an atomic system in which the pump wave is detuned from the atomic resonance by Δ. The absorption spectrum shows that the gain (negative absorption) can occur at a pump–probe detuning Ω_{2L} such that

$$\Omega_{2L} = (\Delta^2 + \Omega_R^2)^{1/2}, \tag{3.9}$$

where $\Omega_R = \mu|E_0|/\hbar$ is the Rabi frequency; Ω_R is sometimes referred to as the generalized Rabi frequency.[34] This phenomenon is understood in terms of the optical Stark effect that leads to a shift of the atomic levels by Ω_{2L} in the presence of the pump field. For $\Delta = 0$, the shift is proportional to $|E_0|$. However, for $\Delta \gg \Omega_R$, the shift becomes linear in the pump intensity $|E_0|^2$, since Ω_{2L} can be approximated by

$$\Omega_{2L} \approx \Delta\left(1 + \frac{\Omega_R^2}{2\Delta^2}\right). \tag{3.10}$$

A comparison of Eq. (3.8) and relation (3.10) shows that semiconductor lasers behave in a manner analogous to that of detuned atomic systems with the effective detuning

$$\Delta = -[(1 + \beta^2)^{1/2} + 1]/(\beta\tau_s). \tag{3.11}$$

The parameter β controls the extent of detuning. For $\beta \gg 1$, $|\Delta| \approx \tau_s^{-1}$. Thus maximum detuning is governed by the spontaneous carrier lifetime.

The analogy between a semiconductor laser and a detuned atomic system suggests that the enhancement of probe gain in the vicinity of Ω_p can be interpreted in terms of the optical Stark effect. The analogy should not, however, be pushed too far. In particular, the concept of the Rabi frequency for a semiconductor laser is not necessarily valid because of the obvious complications arising from the band structure.

4. NEARLY DEGENERATE FOUR-WAVE MIXING

As was mentioned earlier, population pulsations not only affect the probe susceptibility but also are responsible for NDFWM. This can be seen from Eq. (3.1) by noting that the induced polarization at the probe frequency has a contribution arising from the nonlinear interaction between the pump wave and the conjugate wave. Such a contribution couples the probe wave and the conjugate wave and can generate the conjugate wave at $\omega_2 = 2\omega_0 - \omega_1$ even if no field at that frequency is incident upon the semiconductor laser. The study of NDFWM consists of obtaining the coupled-wave equations for the probe wave and the conjugate wave and solving them subject to appropriate boundary conditions at the laser facets. We perform such a procedure in this section.

We substitute Eqs. (2.2) and (2.14) into Eq. (2.1), multiply by $U^*(x, y)$, and integrate over the transverse dimensions x and y. This leads to the one-dimensional wave equation

$$\frac{d^2E_j}{dz^2} + k_j^2E_j = -\frac{\omega_j^2\Gamma}{\epsilon_0c^2}P_j, \tag{4.1}$$

where $k_j = \bar{n}\omega_j/c$ and $\bar{n}$ is the effective mode index corresponding to the waveguide mode $U(x, y)$. The polarization components P_j are given by Eqs. (2.15)–(2.17). The confinement factor Γ appears in Eq. (4.1) since $P_j = 0$ outside the active region of the semiconductor (because $\overline{N} = 0$). Γ accounts for the spatial effects related to the non-plane-wave nature of the interacting waves.

To obtain the coupled-wave equations from Eq. (4.1), we must consider the specific experimental configuration employed for NDFWM. In the case of semiconductor lasers the interaction is collinear[10–12] because of the relatively small dimensions of the active region. In the most general case we must consider the forward and backward components of the pump, probe, and conjugate waves leading to a set of six wave equations coupled by the mixing of the forward and backward components at the partially reflecting laser facets. Such a problem requires numerical solution; the numerical approach is necessary when the semiconductor laser operates in the above-threshold regime. However, the main qualitative features of NDFWM can be obtained in a simpler manner when the semiconductor laser operates below threshold as an amplifier. The analysis is particularly simple if we consider the case of a traveling-wave amplifier whose facets have negligible relectivities (by the use of an antireflection coating). More specifically, we assume that two counterpropagating pump waves are incident at the two facets of an amplifier of length L and that a probe wave (shifted by Ω from the pump-wave frequency) is incident at the left facet at $z = 0$. In the collinear geometry, the pump, probe, and conjugate fields are given, respectively, by

$$E_0 = P_s^{1/2}[E_f(z)\exp(ik_0z) + E_b(z)\exp(-ik_0z)], \quad (4.2)$$

$$E_1 = P_s^{1/2}[A_1(z)\exp(ik_1z)], \quad (4.3)$$

$$E_2 = P_s^{1/2}[A_2(z)\exp(-ik_2z)]. \quad (4.4)$$

The use of Eqs. (4.2)–(4.4) in Eq. (4.1), together with Eqs. (2.15)–(2.17), leads to the following set of equations:

$$\frac{dE_f}{dz} = -\alpha_0 E_f, \qquad \frac{dE_b}{dz} = \alpha_0 E_b, \quad (4.5)$$

$$\frac{dA_1}{dz} = -\alpha_1 A_1 + i\kappa_1 A_2^* \exp(i\Delta kz), \quad (4.6)$$

$$\frac{dA_2^*}{dz} = \alpha_2^* A_2^* + i\kappa_2 A_1 \exp(-i\Delta kz), \quad (4.7)$$

where the pump-wave absorption coefficient is

$$\alpha_0 = -\frac{(1 - i\beta)g_0}{2(1 + P_0)} \quad (4.8)$$

and g_0 is the small-signal gain related to the device current I through Eq. (2.23). The absorption coefficient α_j and the coupling coefficient κ_j are given by

$$\alpha_j = \alpha_0\left(1 - \frac{CP_0}{1 + P_0 \pm i\Omega\tau_s}\right), \quad (4.9)$$

$$\kappa_j = -i\alpha_0\left(\frac{2CE_f(z)E_b(z)}{1 + P_0 \pm i\Omega\tau_s}\right), \quad (4.10)$$

where a plus and a minus are chosen for $j = 2$ and $j = 1$, respectively. In Eqs. (4.6) and (4.7),

$$\Delta k = k_2 - k_1 = -2\bar{n}\Omega/c \quad (4.11)$$

is the wave-number mismatch resulting from the nondegenerate nature of the four-wave mixing process.

In Eqs. (4.8)–(4.10), $P_0 = |\bar{E}_0|^2/P_s$ is the average intracavity pump intensity normalized to the saturation intensity. By using Eq. (4.2), it can be written as

$$P_0 = \frac{1}{L}\int_0^L [|E_f(z)|^2 + |E_b(z)|^2]dz, \quad (4.12)$$

where we have neglected the interference term resulting from spatial hole burning. As mentioned earlier, this is justified for semiconductor lasers, since carrier diffusion tends to wash out the spatial holes in the carrier population burned by the counterpropagating pump waves. The average over the amplifier length L in Eq. (4.12) is a consequence of our assumption of spatially homogeneous carrier density in Eq. (2.8). This assumption can be relaxed by allowing P_0 to be a slowly varying function of z along the amplifier length, but only at the expense of considerable complexity, since Eqs. (4.5)–(4.7) must then be solved numerically. By treating P_0 as independent of z, the coefficients α_j and κ_j are constant, and Eqs. (4.6) and (4.7) can be readily solved.

We can relate P_0 to the incident pump intensity P_{in} by using Eqs. (4.5) and (4.12). If we assume that the pump beams of equal intensity are incident upon the two ends of the amplifier,

$$|E_f(0)|^2 = |E_b(L)|^2 = P_{in}. \quad (4.13)$$

We solve Eq. (4.5) subject to the above boundary conditions and carry out the integration in Eq. (4.12). The result is

$$P_{in} = \frac{g_0L}{2}\frac{P_0}{1 + P_0}\left[\exp\left(\frac{g_0L}{1 + P_0}\right) - 1\right]^{-1}. \quad (4.14)$$

For given values of P_{in} and g_0L, Eq. (4.14) can be used to obtain P_0. Before proceeding with the solution of the coupled-wave equations, we note from Eqs. (4.5) that $E_f(z)E_b(z)$ is constant (z independent) and can be replaced by

$$E_f(z)E_b(z) = P_{in}\exp\left[\frac{g_0L}{2(1 + P_0)}\right] \quad (4.15)$$

in Eq. (4.10) by using Eq. (4.13). Thus both α_j and κ_j are independent of z in the coupled-wave Eqs. (4.6) and (4.7).

Because of their linearity, Eqs. (4.6) and (4.7) can be readily solved. Under typical experimental conditions only the probe wave is incident at $z = 0$, and the conjugate wave is generated without any input. Using the boundary condition $A_2^*(L) = 0$, the conjugate reflectivity R and the probe transmittance T are given by[35,36]

$$R = \left|\frac{A_2^*(0)}{A_1(0)}\right|^2 = \left|\frac{\kappa_2\sin(pL)}{p\cos(pL) + \alpha\sin(pL)}\right|^2, \quad (4.16)$$

$$T = \left|\frac{A_1(L)}{A_1(0)}\right|^2 = \left|\frac{p\exp(-\bar{\alpha}L)}{p\cos(pL) + \alpha\sin(pL)}\right|^2, \quad (4.17)$$

where

$$p = (\kappa_1\kappa_2^* - \alpha^2)^{1/2}, \quad (4.18)$$

$$\alpha = (\alpha_1 + \alpha_2^* + i\Delta k)/2, \quad (4.19)$$

$$\bar{\alpha} = (\alpha_1 - \alpha_2^* - i\Delta k)/2. \quad (4.20)$$

We have studied the variation of R and T with the normalized pump–probe detuning $\Omega\tau_s$ for a range of experimentally accessible parameters. The two parameters that can be experimentally controlled are the small-signal gain g_0 (varied by changing the device current I) and the incident pump intensity P_{in}. The only other parameters that must be specified are the overlap factor C and the linewidth enhancement factor β. We choose $C = 0.5$ and $\beta = 5$ as typical values for InGaAsP lasers. Since $|\Delta kL| \sim 10^{-3}$ from Eq. (4.11) for detunings $|\Omega|\tau_s \sim 1$, the phase mismatch is negligible in the case of nearly degenerate four-wave mixing. The available small-signal gain before the laser reaches threshold depends on the facet reflectivities. If we take $\alpha_{int}L = 1$ and $R_1 = R_2 = 1\%$ in Eqs. (2.20) and (2.21), the threshold is reached for $g_0L = 5.6$; a value of $g_0L \simeq 4$ is easily achieved. In order to relate P_{in} to the actual pump powers, we need an estimate of the saturation power. By using Eq. (12) and assuming a mode cross section of 1 μm^2, we estimate a saturation power of about 5 mW. Thus $P_{in} = 0.2$ corresponds to an incident pump power of 1 mW.

Figure 4 shows the dependence of the reflectivity and transmittance spectra (R and T as functions of $\Omega\tau_s$) on the pump power P_{in} for $g_0L = 4$. The reflectivity spectrum is nearly Lorentzian, and its peak height increases rapidly with P_{in}, reaches a maximum value, and then decreases with a further increase in P_{in} because of the saturation effects. For the parameter values used in Fig. 4, R exceeds 1000 for $P_{in} \simeq$

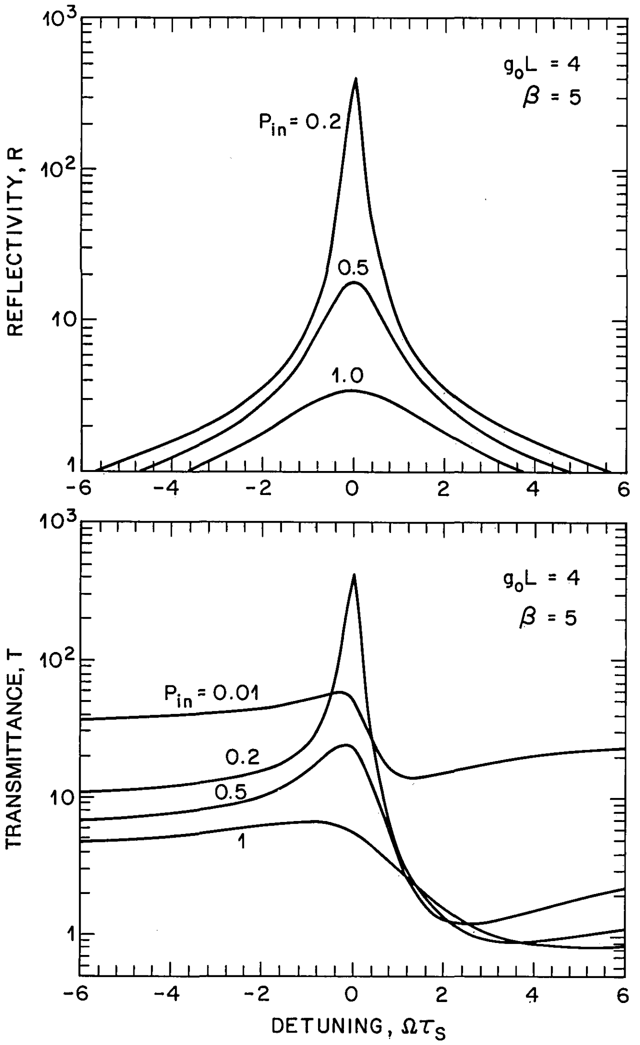

Fig. 4. Variation of the conjugate reflectivity R and the probe transmittance T with the normalized pump–probe detuning $\Omega\tau_s$ for several incident pump intensities when the semiconductor laser operates as a traveling-wave amplifier with $g_0L = 4$.

0.1. A peak reflectivity of about 50 can be obtained even for $P_{in} = 0.01$ (pump power $\simeq 50\ \mu W$) because of the amplifying nature of the nonlinear medium. This is in agreement with the experimental result[12] on a GaAs amplifier where $R = 35$ was observed at a pump power of 70 μW (since the laser facets were uncoated, $g_0L \simeq 2$ in that experiment, rather than the value of 4 assumed here). Higher reflectivities were obtained in a recent experiment[37] with an InGaAsP amplifier whose facets were antireflection coated to increase g_0L. The spectral width of the reflectivity profile can be estimated by using Eqs. (4.10) and (4.16) and by noting that $R \propto |\kappa_2|^2$ at low pump powers. The spectrum is Lorentzian, with a width (FWHM) of[15]

$$\Delta\nu = \frac{1 + P_0}{\pi\tau_s}. \tag{4.21}$$

As expected, the width increases linearly with the pump power because of pump-induced power broadening. Measurements of $\Delta\nu$ can lead to an accurate estimate of the spontaneous carrier lifetime τ_s. Note that τ_s depends on the small-signal gain of the amplifier. This is so because an increase in g_0 increases the steady-state carrier density $\bar{N}$ and reduces τ_s through processes such as Auger recombination.

The transmittance spectra in Fig. 4 show the dependence of probe amplification on the pump-probe detuning. In the absence of population pulsations, $\kappa_1 = 0$ and $\alpha_1 = \alpha_0$. From Eq. (4.8), the probe transmittance T_0 in that case is given by

$$T_0 = \left|\frac{A_1(L)}{A_1(0)}\right|^2 = \exp\left(\frac{g_0L}{1 + P_0}\right). \tag{4.22}$$

Thus, the probe transmittance is expected to be detuning independent in the absence of population pulsations. This is indeed the case in Fig. 4 for $|\Omega\tau_s| \gg 1$. However, considerable enhancement of T_0 can occur when the probe is detuned on the low-frequency side of the pump such that $\Omega = \Omega_p$, where Ω_p is given by Eq. (3.8). An enhancement by a factor of 50 can be seen in Fig. 4 for $P_{in} = 0.2$. The enhancement factor decreases with a further increase in the pump power because of the saturation effects. The physical mechanism behind the enhancement is the one discussed in Section 3 that leads to an enhancement of the probe gain, with a maximum enhancement occurring at Ω_p (see Fig. 1).

As mentioned earlier, both the gain grating and the index

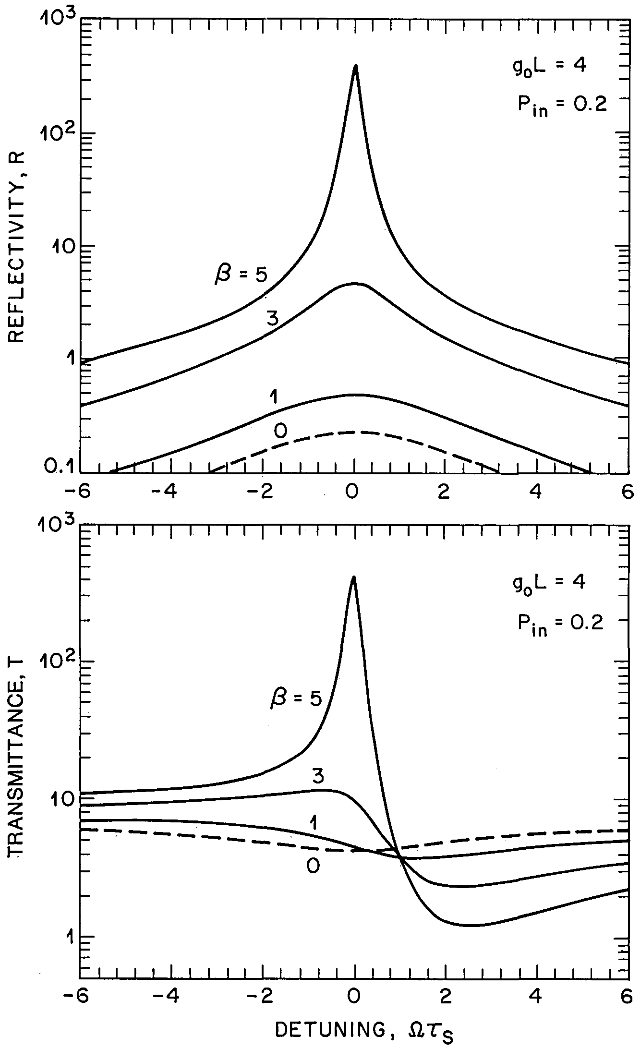

Fig. 5. Same as for Fig. 4 except that the effect of linewidth enhancement factor β on the reflectivity and transmittance spectra is shown at a fixed pump intensity.

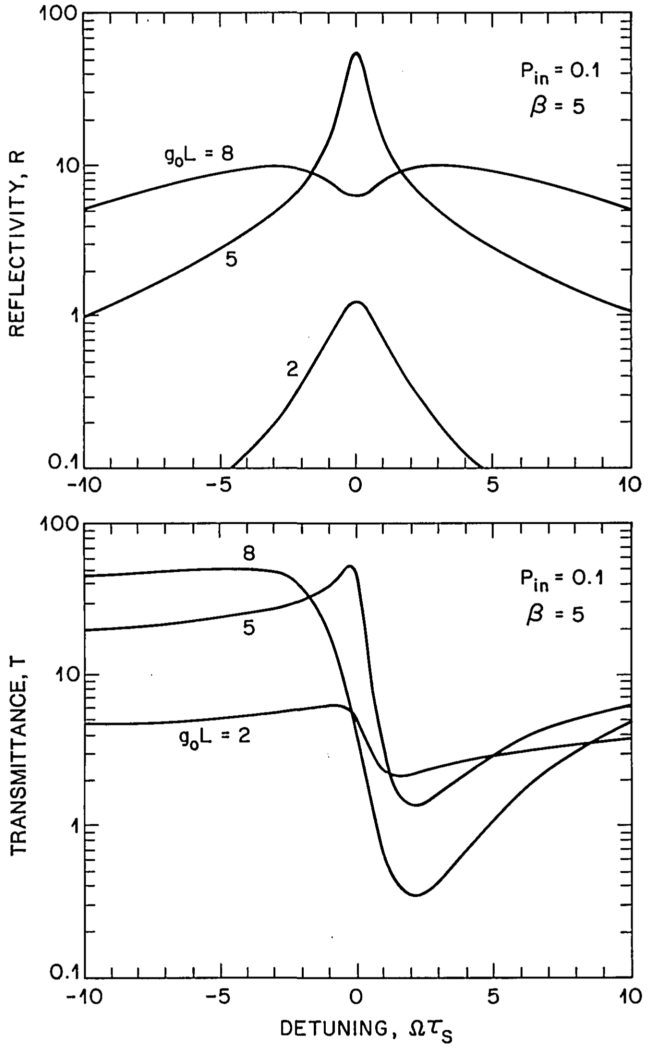

Fig. 6. Same as for Fig. 4 except that the effect of small-signal gain on the reflectivity and transmittance spectra is shown for $P_{in} = 0.1$ and $\beta = 5$.

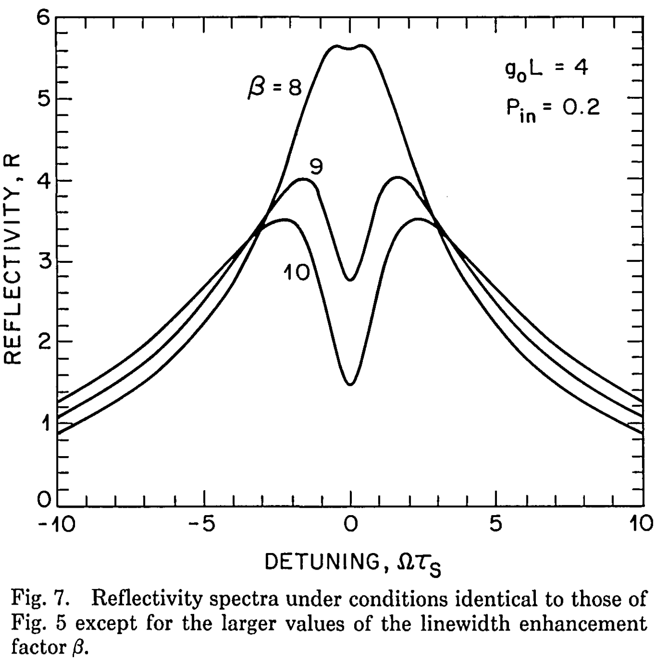

Fig. 7. Reflectivity spectra under conditions identical to those of Fig. 5 except for the larger values of the linewidth enhancement factor β.

grating created by population pulsations contribute to the NDFWM process. The relative contribution of the two gratings is governed by the linewidth enhancement factor β. This is seen more quantitatively in Fig. 5, in which the reflectivity and transmittance spectra are plotted for several values of β with $P_{in} = 0.2$ and $g_0L = 4$. When $\beta = 0$, only the gain grating contributes to the NDFWM process, and the conjugate reflectivity R is relatively small ($R \lesssim 0.2$). However, it increases rapidly with an increase in β; for the parameter values used in Fig. 5, $R \simeq 400$ for $\beta = 5$. Clearly, the index-grating contribution to NDFWM dominates in the case of semiconductor lasers. The same conclusion holds for the transmittance T; the enhancement factor for T in Fig. 5 increases with β. More importantly, the transmittance spectrum is symmetric for $\beta = 0$ (when only the gain grating contributes) and becomes asymmetric for $\beta \neq 0$. Thus the carrier-induced index change is responsible for the asymmetric probe transmission with respect to the pump–probe detuning,[15] as is also evident from Fig. 3. The theoretical prediction of asymmetric probe transmission has been verified in a recent experiment by using an InGaAsP amplifier.[37]

So far we have assumed that $g_0L = 4$. Figure 6 shows the dependence of the reflectivity and transmittance spectra on the small-signal gain for the values $P_{in} = 0.1$ and $\beta = 5$. As is expected, R increases rapidly with an increase in g_0L. However, after a certain value of g_0L, the peak reflectivity decreases, and the spectrum develops a two-peak structure with a central dip. The central dip can occur at lower values of g_0L, but larger values of β are necessary. This is shown in Fig. 7, in which the reflectivity spectra are plotted by using parameter values that are identical to those used for Fig. 5 except for the higher β values in the range 8–10. Although some semiconductor lasers may have such large values of β, typical values of β are in the range 4–6.[29] Thus it appears that an experimental observation of the double-peak reflectivity spectrum would require relatively large values of g_0L, which may be achieved by reducing the facet reflectivities to <1%.

The origin of the central dip in Figs. 6 and 7 can be understood by noting that the variation of R with Ω depends on how $|\kappa_2|$ and $\mathrm{Re}(\alpha)$ vary with the detuning Ω. In particular, a dip can occur at $\Omega = 0$ if $\mathrm{Re}(\alpha)$ is more sharply peaked than $|\kappa_2|$ around $\Omega = 0$.[38] A dip in the reflectivity spectrum can also result from the pump imbalance,[38,39] i.e., when the incident pump powers at the two ends of the amplifiers are different from each other. Considerable structure in the reflectivity spectrum occurs for two-level systems when the pump frequency is detuned from the atomic resonance.[34,36] Semiconductor lasers, in effect, behave as a detuned system, with the parameter β controlling the amount of detuning, in agreement with our discussion in Section 3.

5. HIGHLY NONDEGENERATE FOUR-WAVE MIXING

The four-wave mixing discussed in Section 4 ceases to occur when the pump–probe detuning exceeds a few gigahertz ($\Omega\tau_s \gg 1$). The reason is that the carrier density is unable to respond at time scales much faster than the spontaneous carrier lifetime ($\tau_s \simeq$ 2–3 nsec). As a result, the gain and index gratings created by the population-pulsation mechanism discussed in Section 2 become ineffective for $\Omega \gg \tau_s^{-1}$.

In this section we consider another mechanism of population pulsations that can lead to four-wave mixing even for pump–probe detunings exceeding 100 GHz.[20] The physical mechanism behind highly NDFWM is spectral hole burning manifested as a nonlinear suppression of the optical gain in semiconductor lasers.[22–26] Since spectral hole burning is governed by the intraband relaxation processes occurring at a fast time scale ($T_1 < 1$ psec), the dynamic gratings remain an effective source of NDFWM for beat frequencies up to ~1 THz. The efficiency of the NDFWM process at such high pump–probe detunings is limited by the phase mismatch, in contrast to the case discussed in Section 4, in which it was limited by the carrier lifetime τ_s.

The theoretical description of spectral hole burning requires the density-matrix approach. More specifically, each set of the conduction-band and valence-band states participating in the band-to-band transitions is modeled as a two-level system whose contribution to the induced polarization is calculated with proper consideration of population pulsations resulting from pump–probe beating. The total polarization is obtained by summing over all such contributions and requires a knowledge of the density of states associated with the two bands. Since the procedure is similar to that used for two-level atomic systems[32–36] and has been discussed in detail elsewhere,[23–26] it is described only briefly here. By the method of Kazarinov *et al.*,[24] we assume that the valence-band population remains in thermal equilibrium throughout the nonlinear interaction. This is justified, since the relaxation time T_1 is much shorter for valence-band electrons than for conduction-band electrons because of the higher density of states associated with the valence band. The density-matrix equations are then of the form

$$\frac{\mathrm{d}}{\mathrm{d}t}\rho_{11} + \frac{\rho_{11} - \bar{\rho}_{11}}{T_1} = \frac{\mu}{i\hbar}(\rho_{12} - \rho_{21})E, \tag{5.1}$$

$$\frac{\mathrm{d}}{\mathrm{d}t}\rho_{12} + \left(i\omega_T + \frac{1}{T_2}\right)\rho_{12} = \frac{\mu}{i\hbar}(\rho_{11} - \bar{\rho}_{22})E, \tag{5.2}$$

where μ is the dipole moment and ω_T is the transition frequency. T_1 is the population-relaxation time of conduction-band electrons, and T_2 is the dipole-relaxation time. They have been introduced phenomenologically, as in the case of the Bloch equations.[17] In the case of semiconductor lasers, T_1 and T_2 are governed by the intraband relaxation processes and have typical values of $T_1 \simeq 0.3$ psec and $T_2 \simeq 0.1$ psec.[23–26]

The induced polarization is obtained by summing over all possible band-to-band transitions, i.e.,

$$P = \int \mu(\omega_T)D(\omega_T)(\rho_{12} + \rho_{21})\mathrm{d}\omega_T, \tag{5.3}$$

where $D(\omega_T)$ is the joint density of states per unit volume. In general, the dipole moment μ is also a function of ω_T. To evaluate ρ, we substitute the total field E from Eq. (2.2) in Eqs. (5.1) and (5.2). Because of pump–probe beating, the general solution of Eq. (5.1) is of the form

$$\rho_{11} = \bar{\rho}_{11} + \Delta\rho_{11}(0) + [\Delta\rho_{11}(\Omega)\exp(i\Omega t) + \text{c.c.}]. \tag{5.4}$$

Physically, ρ_{11} represents the occupation probability of the conduction band state participating in the transition (the Fermi factor of the conduction-band electrons), and $\bar{\rho}_{11}$ is its value in thermal equilibrium (in the absence of optical fields). In the presence of a strong pump field, the occupation probability changes: $\Delta\rho_{11}(0)$ is the static change induced by the pump wave alone, whereas $\Delta\rho_{11}(\Omega)$ is the dynamic change induced by the beating of the pump and probe waves at the beat frequency Ω. The situation is similar to that considered in Section 2. Although $\Delta\rho_{11}(\Omega)$ has its origin in population pulsations, it is the intraband population, and not necessarily the actual carrier density, that pulsates. For $|\Omega|\tau_s \lesssim 1$, the carrier-density pulsations considered in Section 2 should also be included by noting that an integration of ρ_{11} over the conduction-band states leads to the carrier density.

The induced polarization P is calculated by using Eqs. (5.2) and (5.4) in Eq. (5.3). The individual polarization components are obtained by expanding P in the form of Eq. (2.14). The final result is[26]

$$P_0 = \epsilon_0[\chi_L(\omega_0) + \chi_1(0)]E_0, \tag{5.5}$$

$$P_1 = \epsilon_0[\chi_L(\omega_1) + \chi_1(\Omega) + \chi_2(\Omega)]E_1 + \epsilon_0\chi_3(\Omega)E_2^*, \tag{5.6}$$

$$P_2 = \epsilon_0[\chi_L(\omega_2) + \chi_1(-\Omega) + \chi_2(-\Omega)]E_2 + \epsilon_0\chi_3(-\Omega)E_1^*, \tag{5.7}$$

where the linear susceptibility

$$\chi_L(\omega_j) = -\frac{nc}{\omega_j}(\beta + i)g(\bar{N}, \omega_j) \tag{5.8}$$

has a form similar to that of Eq. (2.5). The gain $g(\bar{N}, \omega_j)$ is determined by the current applied to the semiconductor laser. Because of a large frequency difference among pump, probe, and conjugate waves, it is necessary to account for the gain roll-off. If we assume a parabolic gain profile, then

$$g(\bar{N}, \omega_j) = g(\bar{N})[1 - (\omega_p - \omega_j)^2/\Delta\omega_g^2], \tag{5.9}$$

where $g(\bar{N})$ is the peak gain occurring at ω_p and is related to the device current I by Eq. (2.19). $\Delta\omega_g$ is the half-width of the gain profile. The nonlinear contributions χ_1, χ_2, and χ_3 to the susceptibility arise from the pump-induced change in the intraband population, given by Eq. (5.4). More specifically, χ_1 is due to static change $\Delta\rho_{11}(0)$, while χ_2 and χ_3 have their origin in the population-pulsation term $\Delta\rho_{11}(\Omega)$. Their explicit expressions are[24,26]

$$\chi_1(\Omega) = \frac{inc}{\omega_0}\frac{g(\bar{N})C(1 - i\bar{\beta})}{(1 - i\Omega T_2/2)}\frac{|E_0|^2}{\bar{P}_s}, \tag{5.10}$$

$$\chi_2(\Omega) = \frac{inc}{\omega_0}\frac{g(\bar{N})C(1 - i\bar{\beta})}{(1 - i\Omega T_2/2)(1 - i\Omega T_1)}\frac{|E_0|^2}{\bar{P}_s}, \tag{5.11}$$

$$\chi_3(\Omega) = \frac{inc}{\omega_0}\frac{g(\bar{N})C[1 - i\bar{\beta}(1 - i\Omega T_2)]}{(1 - i\Omega T_2)(1 - i\Omega T_1)}\frac{E_0^2}{\bar{P}_s}, \tag{5.12}$$

where $g(\bar{N})$ is the saturated gain given by Eq. (2.24),

$$\bar{P}_s = \hbar^2/(\mu^2 T_1 T_2) \tag{5.13}$$

is the saturation intensity, and the parameter

$$\bar{\beta} = \frac{1}{g_0 T_2}\left(\frac{\mathrm{d}g}{\mathrm{d}\omega}\right)_{\omega=\omega_0} \tag{5.14}$$

is related to the slope of the gain profile at the pump frequency. The overlap factor

$$C = \frac{1}{\Gamma} \int_0^w \int_0^d |U(x, y)|^4 \mathrm{d}x\mathrm{d}y \tag{5.15}$$

results from the spatial structure of the waveguide mode.

Several simplifications were made in the derivation of Eqs. (5.5)–(5.7), the most important being the use of third-order perturbation theory. This is justified, since the saturation intensity $\overline{P}_s$ in Eq. (5.13) is $\simeq 10$ MW/cm^2, in contrast to that used in Section 2, $P_s \simeq 0.5$ MW/cm^2. The integration over ω_T in Eq. (5.3) was performed by assuming that the dominant contribution to the integral comes from a region of width $|\omega_T - \omega_0| = T_2^{-1}$ centered at the pump frequency ω_0. Finally, it was assumed that the transition dipole moment μ and the saturation intensity $\overline{P}_s$ do not vary significantly over this range of integration.

The polarization components P_j given by Eqs. (5.5)–(5.7) can be used in the wave equation [Eq. (4.1)] to discuss NDFWM. We obtain the coupled-wave equations for the probe and conjugate waves that are identical to Eqs. (4.5)–(4.7) but with different absorption coefficients α_j and coupling coefficients κ_j. More specifically,

$$\alpha_0 = -\frac{g_0}{2(1 + P_0)} [1 - i\beta - (1 - i\bar{\beta})CrP_0], \tag{5.16}$$

$$\alpha_1 = -\frac{g_0}{2(1 + P_0)} \left[1 - i\beta - \frac{\Omega^2}{\Delta\omega_g^2} - \frac{(1 - i\bar{\beta})CrP_0}{1 - i\Omega T_2/2} \times \left(1 + \frac{1}{1 - i\Omega T_1}\right)\right], \tag{5.17}$$

$$\kappa_1 = \frac{ig_0}{2(1 + P_0)} \frac{Cr[1 - i\bar{\beta}(1 - i\Omega T_2)]}{(1 - i\Omega T_2)(1 - i\Omega T_1)} 2E_f(z)E_b(z). \tag{5.18}$$

The expressions for α_2 and κ_2 are obtained by changing Ω to $-\Omega$ in Eqs. (5.17) and (5.18). P_0 is given by Eq. (3.4), and the parameter $r = P_s/\overline{P}_s$. The conjugate reflectivity R and the probe transmissivity T are obtained by using Eqs. (4.15)–(4.20) with α_j and κ_j as given by Eqs. (5.17) and (5.18).

Before discussing the spectral features of R and T, we consider the effect of population pulsations on the probe gain. Consider first self-saturation of the pump gain. From Eq. (5.16) we note that the pump gain is saturated by two mechanisms. Interband processes lead to the well-known reduction by a factor of $1 + P_0$. However, intraband processes lead to a further reduction by a factor of $1 - CrP_0$. This effect is known as spectral hole burning; the intense pump wave burns a hole of width T_2^{-1} in the gain profile, as is shown by Eq. (5.10). Typically the gain is reduced by 0.5–1% per milliwatt of the operating power for a semiconductor laser.[26] This information can be used to estimate the saturation power $\overline{P}_s$ instead of using Eq. (5.13). We estimate that $\overline{P}_s$ = 100 mW for index-guided lasers. If we assume that P_s = 5 mW, r = 0.05. Equation (5.16) shows that the refractive index is also changed by a relative amount of $\bar{\beta}CrP_0/\beta$. We can estimate $\bar{\beta}$ by using Eqs. (5.9) and (5.14):

$$\bar{\beta} = \frac{2(\omega_0 - \omega_p)}{T_2\Delta\omega_g^2} \simeq 2(\omega_0 - \omega_p)T_2, \tag{5.19}$$

for which we assume that $\Delta\omega_g \simeq T_2^{-1}$. When the pump frequency ω_0 coincides with the gain at ω_p, $\bar{\beta} = 0$. This is the case for Fabry–Perot-type semiconductor lasers. When the laser is operated as an amplifier, ω_0 may differ from ω_p. However, in most situations of practical interest, $\bar{\beta} \ll 1$. In the following discussion we therefore set $\bar{\beta} = 0$.

The probe gain is calculated from Eq. (5.17) by using $g = -2\,\mathrm{Re}(\alpha_1)$. It is given by

$$g_p = \frac{g_0}{1 + P_0} \left\{1 - \frac{\Omega^2}{\Delta\omega_g^2} - \frac{CrP_0}{1 + (\Omega T_2/2)^2} \times \left[1 + \frac{1 - \Omega^2 T_1 T_2/2}{1 + (\Omega T_1)^2}\right]\right\}. \tag{5.20}$$

In the absence of the pump wave ($P_0 = 0$), $g_p = g_0(1 - \Omega^2/\Delta\omega_g^2)$ is the small-signal probe gain. Equation (5.20) shows that this gain is reduced by spectral hole burning and the saturation effects produced by the pump field. The reduction resulting from population pulsations is given by the last

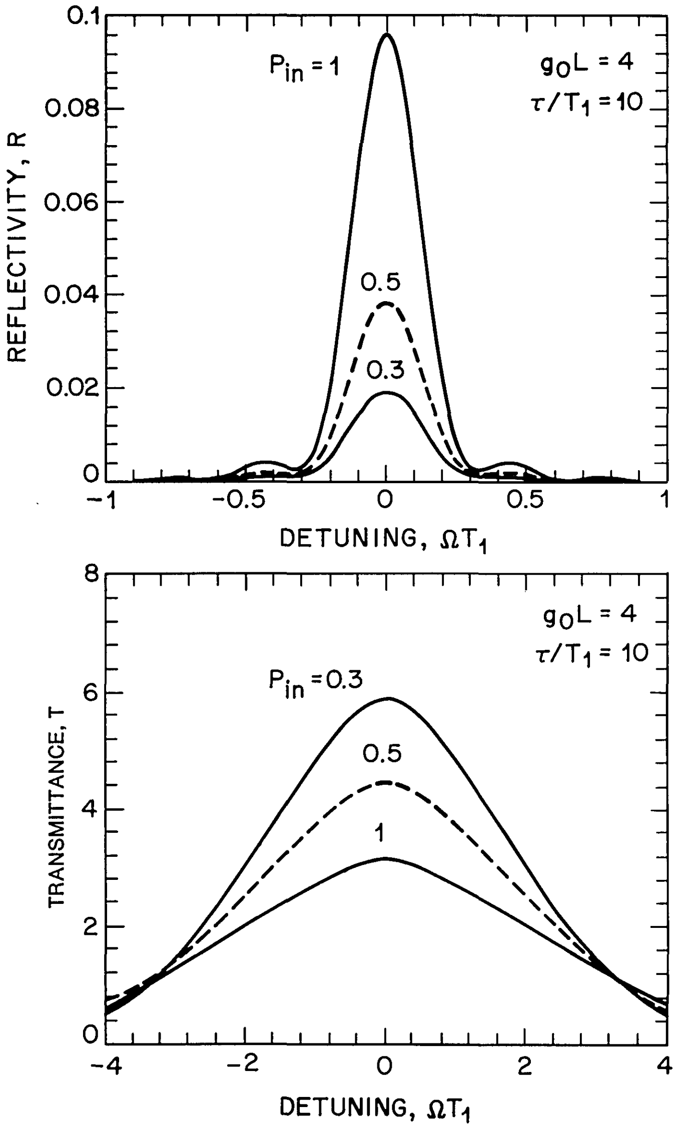

Fig. 8. Reflectivity and transmittance spectra for the case of highly nondegenerate four-wave mixing resulting from spectral hole burning. Pump–probe detuning is normalized to the intraband population-relaxation time T_1. For T_1 = 0.3 psec, ΩT_1 = 1 corresponds to a detuning of about 500 GHz. Other parameters are T_2/T_1 = 1/3 and τ/T_1 = 10.

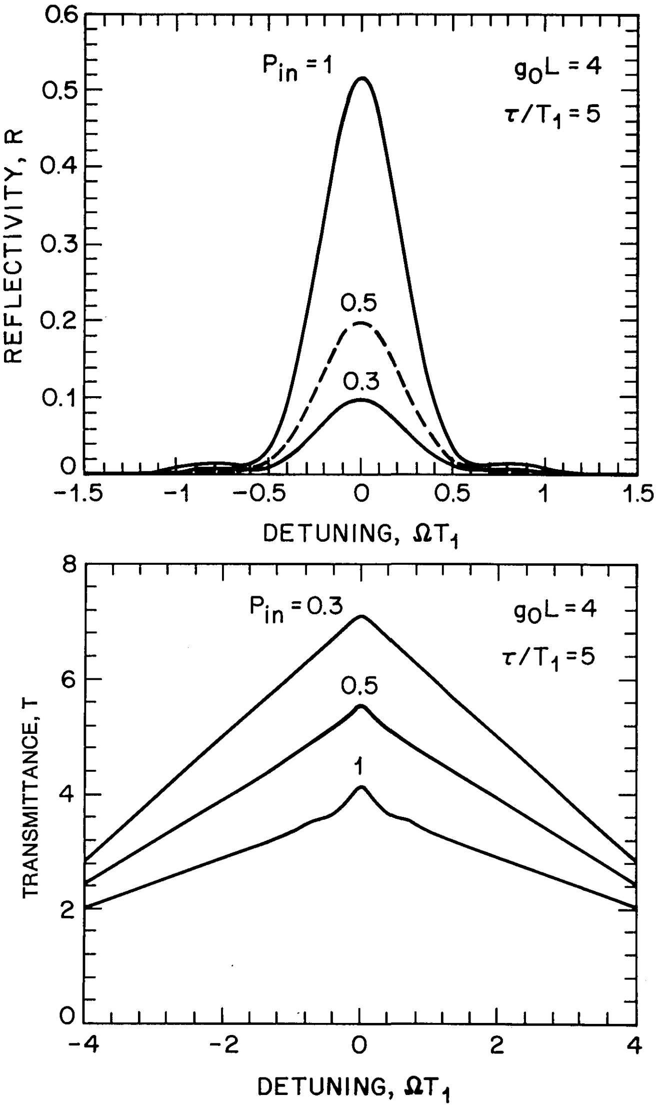

Fig. 9. Same as for Fig. 8 except that the population-relaxation time T_1 has been doubled. As a result, $T_2/T_1 = 1/6$ and $\tau/T_1 = 5$.

term in Eq. (5.20). As is expected, the population-pulsation contribution vanishes for $|\Omega|T_1 \gg 1$. Although population pulsations can change the probe gain by 100% or more for the case discussed in Section 3, such changes are ~1% because of the large saturation power associated with the spectral hole-burning phenomenon. Even such small changes can nonetheless lead to significant NDFWM, as is discussed below.

As in the case discussed in Section 4, we assume that the semiconductor laser is operating as a traveling-wave amplifier with the incident pump intensity P_{in} at the two facets. The intracavity pump intensity P_0 is related to P_{in} by Eq. (4.14). The other parameters are chosen to be $T_1 = 0.3$ psec, $T_2 = 0.1$ psec, $\beta = 5$, $r = 0.05$, and $C = 0.7$. This value of C was estimated by using a Gaussian mode profile in Eq. (5.15).[26] Figure 8 shows the variation of R and T with ΩT_1 for $g_0L = 4$. The phase mismatch is $\Delta kL = -2\Omega\tau$ from Eq. (4.11), where $\tau = \bar{n}L/c$ is the transit time; we chose $\tau/T_1 = 10$. For $T_1 = 0.3$ psec, this corresponds to $\tau = 3$ psec, a typical value for 250-μm-long laser amplifiers.

Figure 8 shows that $R \simeq 0.1$ for $P_{in} = 1$. This should be compared with Fig. 4, for which $R > 100$ even for $P_{in} = 0.2$. Clearly, NDFWM is much less efficient when the nonlinearity is due to pulsations of the intraband population rather than when it is due to modulation of the actual carrier density. This can be understood by comparing the saturation powers P_s and $\bar{P}_s$ associated with the two nonliner mechanisms. As seen from Eq. (5.18), the coupling coefficients κ_j are smaller by a factor of $r = P_s/\bar{P}_s$ for the case of spectral hole burning compared with those obtained from Eq. (4.10). Since $R \propto |\kappa_2|^2$, the reflectivities are expected to be smaller by a factor of r^2. Since $r = 0.05$ in Fig. 8, one can expect that R will be lower by nearly 3 orders of magnitude compared with the values shown in Fig. 4. Note that $\bar{P}_s$, and hence r, depends on the intraband relaxation times T_1 and T_2, which are not precisely known. To show how R and T are affected by an increase in T_1, Fig. 9 shows R and T for the same parameters used for Fig. 8 except for T_1, which was taken to be $T_1 = 0.6$ psec. As expected, R increases to about 0.5. A slight enhancement of T is apparent in the central region because of NDFWM; this enhancement is too small to be evident in Fig. 8. The conjugate reflectivity R can be increased considerably by increasing the amplifier gain g_0L. In particular, R exceeds unity for $g_0L > 6$. Such values of the small-signal gain can be obtained by reducing the residual facet reflectivities to <1%.

An important feature of Figs. 8 and 9 is that the reflectivity profile is narrower than T_1^{-1}. Even though the gain and index gratings are expected to remain effective sources of NDFWM up to $|\Omega|T_1 \sim 1$, the mixing efficiency drops significantly for such large detunings because of the phase mismatch. In other words, the width of the reflectivity spectrum is determined by the transit time τ rather than the population-relaxation time T_1. Since $\tau \simeq 3$ psec for a 250-μm-long semiconductor laser, significant values of R can be obtained for pump–probe detunings up to $\sim\tau^{-1} \simeq 300$ GHz. This range can be extended further by reducing the laser length. The weak satellite peaks in the reflectivity spectra in Figs. 8 and 9 are also due to the phase mismatch.

6. SUMMARY

In this paper we have presented the theory of NDFWM in semiconductor lasers with particular emphasis on the physical processes that lead to population pulsations. Two rather different mechanisms are involved in the NDFWM process, depending on the detuning Ω between the pump wave and the probe wave. For small detunings ($\lesssim 1$ GHz), modulation of the carrier density at the beat frequency Ω creates a dynamic population grating whose effectiveness is governed by the spontaneous carrier lifetime τ_s. This was the physical mechanism involved in the experiments on NDFWM reported in Refs. 10–12 and 37.

For large detunings, such that $|\Omega|\tau_s \gg 1$, the above mechanism cannot generate the conjugate wave, as the carrier density is unable to respond to such high beat frequencies. In that situation a weaker nonlinear effect arising from spectral hole burning can nonetheless lead to significant conjugate reflectivities. Population pulsations in this case refer to modulation of the intraband population, and the effectiveness of the resulting population grating is determined by the intraband population-relaxation time T_1 (~0.3 psec). Our results show that the NDFWM process is limited by the phase mismatch or the transit time τ rather than by the population-relaxation time T_1. For a 250-μm-long semiconductor laser, $\tau \simeq 3$ psec, and significant NDFWM is expected to occur for pump–probe detunings of up to τ^{-1} ($\simeq$300 GHz). Experiments have not yet been performed to observe four-wave mixing under such highly nondegenerate conditions.

The NDFWM process discussed here may have applications in many fields. The highly efficient nature of NDFWM in semiconductor lasers should be useful in the fields of phase conjugation and nonlinear spectroscopy. NDFWM can also be used to stabilize external-cavity semiconductor lasers by providing the feedback from a semiconductor laser operating as a phase-conjugate mirror.[40] In the field of coherent optical communications, semiconductor-laser amplifiers are being proposed to amplify several channels simultaneously. The carrier-density modulation and the resulting NDFWM would then induce interchannel cross talk that would limit the interchannel spacing in such systems.[41] Further work is needed to clarify the role of NDFWM in optical communication systems.

REFERENCES AND NOTES

1. See various chapters in R. A. Fisher, ed., *Optical Phase Conjugation*(Academic, New York, 1983).
2. Special issue on dynamic gratings and four-wave mixing, IEEE J. Quantum Electron. **QE-22,** 1194–1542 (1986).
3. Y. R. Shen, *The Principles of Nonlinear Optics* (Wiley, New York, 1984), Chap. 14.
4. E. E. Bergmann, I. J. Bigio, B. J. Feldman, and R. A. Fisher, "High-efficiency pulsed 10.6-μm phase-conjugate reflection via degenerate four-wave mixing," Opt. Lett. **3,** 82–84 (1978).
5. G. P. Agrawal and C. Flytzanis, "Bistability and hysteresis in phase-conjugated reflectivity," IEEE J. Quantum Electron. **QE-17,** 374–380 (1981).
6. G. P. Agrawal, "Intracavity resonant degenerate four-wave mixing: bistability in phase conjugation," J. Opt. Soc. Am. **73,** 654–660 (1983).
7. A. Tomita, "Phase conjugation using gain saturation of a Nd:YAG laser," Appl. Phys. Lett. **34,** 463–464 (1979).
8. R. A. Fisher and B. J. Feldman, "On resonant phase conjugate reflection and amplification at 10.6 μm in inverted CO_2," Opt. Lett. **4,** 140–152 (1979).
9. J. Reintjes and L. J. Palumbo, "Phase conjugation in saturable amplifiers by degenerate frequency mixing," IEEE J. Quantum Electron. **QE-18,** 1934–1940 (1982).
10. H. Nakajima and R. Frey, "Observation of bistable reflectivity of a phase-conjugated signal through intracavity nearly degenerate four-ware mixing," Phys. Rev. Lett. **54,** 1798–1801 (1985).
11. H. Nakajima and R. Frey, "Intracavity nearly degenerate four-wave mixing in a (GaAl)As semiconductor laser," Appl. Phys. Lett. **47,** 769–771 (1985).
12. H. Nakajima and R. Frey, "Collinear nearly degenerate four-wave mixing in intracavity amplifying media," IEEE J. Quantum Electron. **QE-22,** 1349–1354 (1986).
13. R. Frey, "On-axis intracavity nearly degenerate four-wave mixing in semiconductor lasers," Opt. Lett. **11,** 91–93 (1986).
14. N. C. Kothari and R. Frey, "Bistable behavior of pump, probe, and conjugate signals through collinear intracavity nearly degenerate four-wave mixing," Phys. Rev. A **34,** 2013–2025 (1986).
15. G. P. Agrawal, "Four-wave mixing and phase conjugation in semiconductor laser media," Opt. Lett. **12,** 260–262 (1987).
16. W. E. Lamb, Jr., "Theory of an optical maser," Phys. Rev. A **134,** 1429–1450 (1964).
17. M. Sargent III, M. O. Scully, and W. E. Lamb, Jr., *Laser Physics* (Addison-Wesley, Reading, Mass., 1974), Chap. 9.
18. S. T. Hendow and M. Sargent III, "Theory of single-mode laser instabilities," J. Opt. Soc. Am. B **2,** 84–101 (1985).
19. A. P. Bogatov, P. G. Eliseev, and B. N. Sverdlov, "Anomalous interaction of spectral modes in a semiconductor laser," IEEE J. Quantum Electron. **QE-11,** 510–515 (1975).
20. G. P. Agrawal, "Highly nondegenerate four-wave mixing in semiconductor lasers due to spectral hole-burning," Appl. Phys. Lett. **51,** 302–304 (1987).
21. Y. Nishimura and Y. Nishimura, "Spectral hole-burning and nonlinear-gain decrease in a band-to-level transition semiconductor laser," IEEE J. Quantum Electron. **QE-9,** 1011–1019 (1973).
22. B. Zee, "Broadening mechanism in semiconductor (GaAs) lasers: limitations to single mode power emission," IEEE J. Quantum Electron. **QE-14,** 727–736 (1978).
23. M. Yamada and Y. Suematsu, "Analysis of gain suppression in undoped injection lasers," J. Appl. Phys. **52,** 2653–2664 (1981).
24. R. F. Kazarinov, C. H. Henry, and R. A. Logan, "Longitudinal mode self-stabilization in semiconductor lasers," J. Appl. Phys. **53,** 4631–4644 (1982).
25. M. Asada and Y. Suematsu, "Density-matrix theory of semiconductor lasers with relaxation broadening model—gain and gain-suppression in semiconductor lasers," IEEE J. Quantum Electron. **QE-21,** 434–442 (1985).
26. G. P. Agrawal, "Gain nonlinearities in semiconductor lasers: theory and application to distributed feedback lasers," IEEE J. Quantum Electron. **QE-23,** 860–868 (1987).
27. G. P. Agrawal and N. K. Dutta, *Long-Wavelength Semiconductor Lasers* (Van Nostrand Reinhold, New York, 1986).
28. C. H. Henry, "Theory of the linewidth of semiconductor lasers," IEEE J. Quantum Electron. **QE-18,** 259–264 (1982).
29. M. Osinski and J. Buus, "Linewidth broadening factor in semiconductor lasers—an overview," IEEE J. Quantum Electron. **QE-23,** 9–29 (1987).
30. The expression for ΔN in Ref. 15 is in error. However, this does not affect the conclusions reported therein.
31. B. R. Mollow, "Stimulated emission and absorption near resonance for driven systems," Phys. Rev. A **5,** 2217–2222 (1982).
32. F. Y. Wu, S. Ezekiel, M. Ducloy, and B. R. Mollow, "Observation of amplification in a strongly driven two-level atomic system at optical frequencies," Phys. Rev. Lett. **38,** 1077–1080 (1977).
33. M. Sargent III, "Spectroscopic techniques based on Lamb's laser theory," Phys. Rep. **43,** 223–265 (1978).
34. R. W. Boyd, M. G. Raymer, P. Narum, and D. J. Harter, "Four-wave parametric interaction in a strongly driven two-level system," Phys. Rev. A **24,** 411–423 (1981).
35. T. Fu and M. Sargent III, "Effect of signal detuning on phase conjugation," Opt. Lett. **4,** 366–368 (1979).
36. D. J. Harter and R. W. Boyd, "Nearly degenerate four-wave mixing enhanced by the ac Stark effect," IEEE J. Quantum Electron. **QE-16,** 1126–1131 (1980).
37. K. Inoue, T. Mukai, and T. Saitoh, "Nearly degenerate four-wave mixing in a traveling-wave semiconductor laser amplifier," Appl. Phys. Lett. **51,** 1051–1053 (1987).
38. J. Nilsen and A. Yariv, "Nondegenerate four-wave mixing in a homogeneously broadened two-level-system with saturating pump waves," IEEE J. Quantum Electron. **QE-18,** 1947–1952 (1982).
39. G. P. Agrawal, A. Van Lerberghe, P. Aubourg, and J. L. Boulnois, "Saturation splitting in the spectrum of resonant degenerate four-wave mixing," Opt. Lett. **7,** 540–542 (1982).
40. K. Vahala, K. Kyuma, A. Yariv, S.-K. Kwonk, M. Cronin-Golomb, and K. Y. Lau, "Narrow linewidth, single frequency semiconductor laser with a phase-conjugate external-cavity mirror," Appl. Phys. Lett. **49,** 1563–1565 (1986).
41. G. P. Agrawal, "Amplifier-induced crosstalk in multichannel coherent lightwave systems," Electron. Lett. **23,** Oct 23 (1987).

Govind P. Agrawal

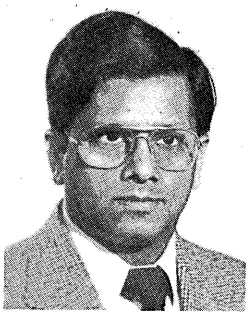

Govind P. Agrawal was born in Kashipur, India, on July 24, 1951. He received the M.S. and Ph.D. degrees in physics from the Indian Institute of Technology, New Delhi, in 1971 and 1974, respectively. After spending several years at the Ecole Polytechnique, France, the City University of New York, and Quantel, France, he joined AT&T Bell Laboratories in 1982 as a member of the technical staff. His research interests have been in the fields of quantum electronics, nonlinear optics, and laser physics. He is an author or coauthor of more than 100 research papers and a book entitled *Long-Wavelength Semiconductor Lasers*. Currently he is engaged in the research and development of semiconductor lasers. Dr. Agrawal is a member of the American Physical Society, a senior member of the Institute of Electrical and Electronics Engineers, and a Fellow of the Optical Society of America.